ACS APPLIED MATERIALS & INTERFACES

Research Article

www.acsami.org

Fabrication and Characteristics of GaN-Based Light-Emitting Diodes with a Reduced Graphene Oxide Current-Spreading Layer

Beo Deul Ryu,[†] Min Han,[†] Nam Han,[†,‡] Young Jae Park,[†] Kang Bok Ko,[†] Tae Hyun Lim,[†] S. Chandramohan,[†] Tran Viet Cuong,[†] Chel-Jong Choi,[†] Jaehee Cho,[†] and Chang-Hee Hong*[,†]

[†]School of Semiconductor and Chemical Engineering, Semiconductor Physics Research Center, Chonbuk National University, Jeonju, 561-756, South Korea

[‡]Department of Materials Science and Engineering, Pohang University of Science and Technology, Pohang 790-784, South Korea

Supporting Information

ABSTRACT: A reduced graphene oxide (GO) layer was produced on undoped and n-type GaN, and its effect on the current- and heat-spreading properties of GaN-based light-emitting diodes (LEDs) was studied. The reduced GO inserted between metal electrode and GaN semiconductor acted as a conducting layer and enhanced lateral current flow in the device. Especially, introduction of the reduced GO layer on the n-type GaN improved the electrical performance of the device, relative to that of conventional LEDs, due to a decrease in the series resistance of the device. The enhanced current-spreading was further of benefit, giving the device a higher light output power and a lower junction temperature at high injection currents. These results therefore indicate that reduced GO can be a suitable current and heat-spreading layer for GaN-based LEDs.

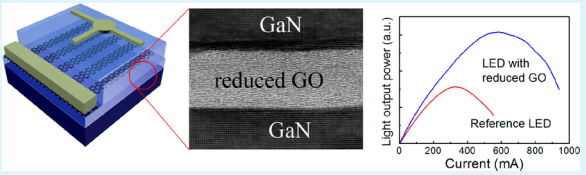

KEYWORDS: *graphene oxide, thermal reduction, reduced graphene oxide, GaN, light-emitting diode, current-spreading layer*

1. INTRODUCTION

The study of high-performance GaN-based light-emitting diodes (LEDs) is very important because LEDs are a potential alternative light source for various applications, including full color displays, backlights of liquid crystal displays, and general illumination.[1,2] In order to make them suitable for use in next-generation solid-state lighting, the LEDs are expected to be able to operate at a high injection current. However, current crowding and efficiency droop are two technical issues that hinder the use of the device in high injection current applications.[3,4] Current crowding occurs near the edge of the mesa in the side-by-side contacts of GaN-based LEDs grown on an insulating sapphire substrate. This is caused by the fact that the resistivity of n-type GaN (~0.01 Ω·cm) is limited by epitaxial growth restraints. This phenomenon can be understood by considering the current-spreading length dependence on the injected current density inside the LED, such that the current density decreases exponentially as the distance increases from the mesa edge at high injection currents.[3,5,6] In addition, current crowding has a strong influence on the charge separation in the quantum wells, limiting the internal quantum efficiency.[7] Although vertical-type LED configurations have been adopted to solve the issues mentioned above, rather poor processes such as complicated wafer bonding and laser lift-off result in a low yield relative to that of lateral-configuration LEDs.

Two-dimensional (2D), single-atom-thick, sp^2-hybridized graphene is an attractive material for use in energy applications owing to its extraordinary mechanical, electrical, optical, and thermal properties.[8] Recently, Yan et al.[9] reported on an improved heat-spreading channel implemented with a graphene layer on a GaN transistor. Furthermore, since graphene is a highly transparent conducting material, it has been exploited as a transparent conducting layer in GaN-based LEDs.[10] However, full utilization of the unique optoelectronic properties of graphene is often impeded by the drawback of several fabrication processes such as a low transfer yield of large-scale graphene to target substrates, difficulty in processing, poor surface cleanliness, etc. Solution-based synthesis of graphene has become a promising alternative to chemical vapor deposition (CVD)-grown graphene, because graphene of any desired size can be directly obtained through chemical/thermal conversion of graphene oxide (GO) coatings.[11,12] GO can be mass-produced and processed in solution at a relatively low cost, making it attractive for use in large-scale applications. In addition, GO's optical and electrical properties can be tuned through a reduction process.[13,14] As an example, the conductivity of reduced GO can be improved by removing functional oxygen groups, and a resistivity value of $\sim 10^{-3}$ to 10 Ω·cm can be achieved through various reduction methods, as reported in a previous study.[15] Reduced GO, therefore, has the potential to be implemented in a wide variety of semiconductor electronic devices, such as the electrodes of UV detectors[16] and solar cells.[17]

Received: September 21, 2014
Accepted: November 20, 2014
Published: November 20, 2014

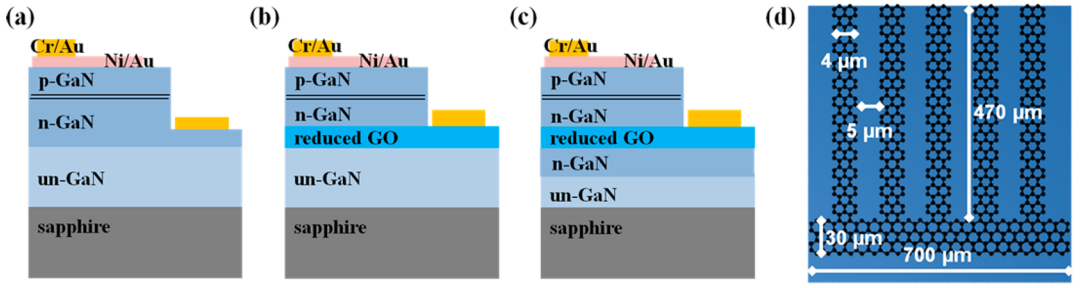

Figure 1. Schematic diagrams of cross-sectional views of (a) conventional LED, (b) sample A, and (c) sample B, and (d) top view of the reduced GO layer structure used in samples A and B.

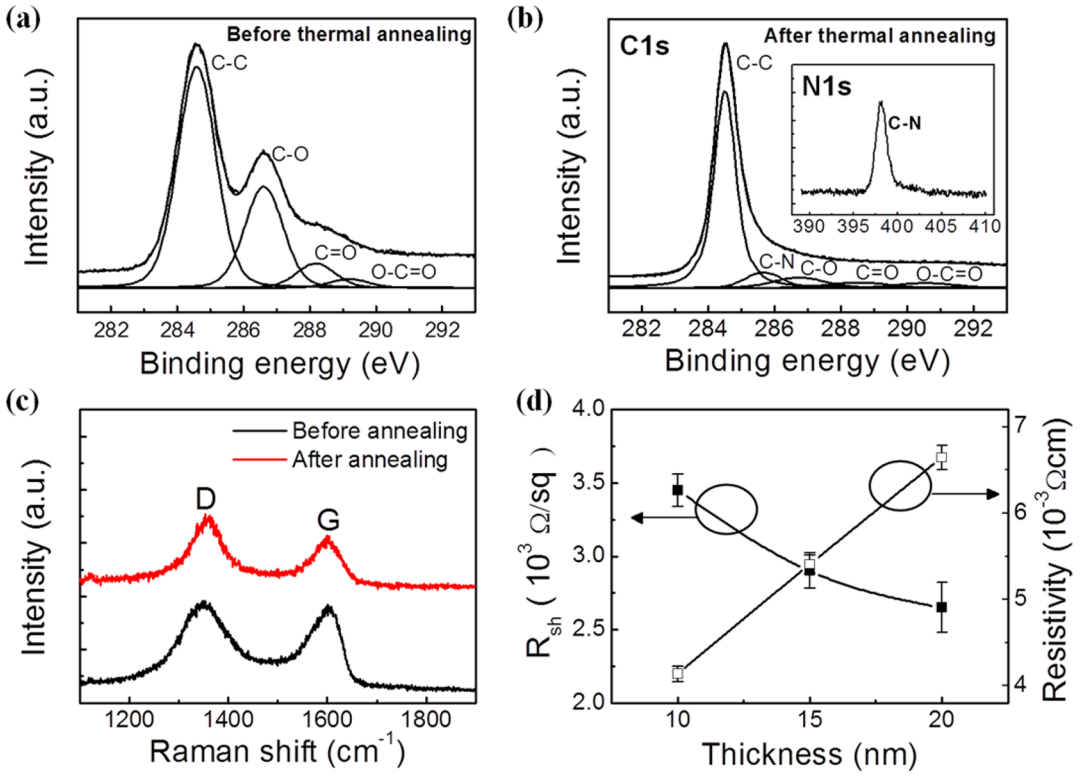

Figure 2. High-resolution XPS C 1s spectra of the GO sheets (a) before and (b) after thermal annealing. (Inset) High-resolution N 1s spectrum of reduced GO sheets. (c) Raman spectra of the GO sheet before and after thermal annealing. (d) Sheet resistance and electrical resistivity of reduced GO with different thicknesses after thermal annealing.

The purpose of this study is to investigate the role of embedded reduced GO current-spreading layer in GaN-based LED devices. It is found that reduced GO coated on undoped and n-type GaN enhanced the lateral current transfer at high injection currents. By embedding reduced GO selectively in the n-type GaN layer in an LED, it is possible to decrease the device series resistance. A prototype LED was fabricated with a reduced GO layer acting as a current spreader for electrons, and this prototype LED offered the lowest series resistance and junction temperature with the highest optical output power.

2. EXPERIMENTAL SECTION

2.1. Formation of Reduced Graphene Oxide. The performance characteristics of the reduced GO were investigated in order to apply it as a current-spreading layer in GaN-based LEDs. The GO dispersion (500 mg/L concentration; Graphene Supermarket, New York) was spray-coated on a GaN substrate as well as a SiO_2/Si substrate for film characterization. Then, to remove the oxygen functional groups, the GO sheets were thermally annealed in mixed hydrogen and ammonia atmosphere (the hydrogen/ammonia ratio was ~2) at 1070 °C for 10 min.

2.2. Device Fabrication. Two types of GaN-based LED devices, noted as samples A and B, along with a conventional LED (Figure 1a) were fabricated in order to investigate the effects of reduced GO on current spreading. The difference between samples A and B is that the GO dispersion was spray-coated on 2-μm undoped GaN or 1-μm Si-doped n-type GaN, respectively, as described in Figure 1b,c. The undoped and n-type GaN epitaxial layers were grown on a *c*-plane (0001) sapphire substrate via metal−organic chemical vapor deposition (MOCVD). Subsequently, a thin GO stripe pattern of given dimension (Figure 1d) was fabricated by standard photolithography processes. Before the subsequent growth of the LED epilayers, a 100 nm-thick SiO_2 film was deposited onto the top of the GO pattern via plasma-enhanced chemical vapor deposition (PECVD) in order to protect the GO from being completely covered by the epilayers. Only a part of the GO pattern with an area of 30 μm × 700 μm was covered by SiO_2, and SiO_2 from all other regions was etched by use of a buffered oxide etchant. Then the prepared samples were loaded again into the MOCVD chamber for thermal reduction and n-type doping in hydrogen and ammonia atmosphere at 1070 °C. Then,

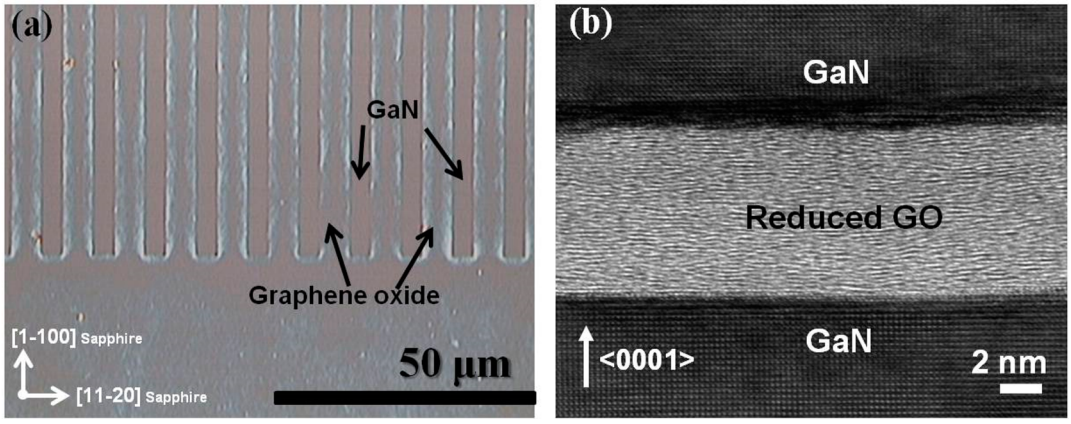

Figure 3. (a) Optical microscopic image of reduced GO layer on a sapphire substrate after thermal annealing. (b) Cross-sectional bright-field HR-TEM image of GaN/reduced GO/GaN interface.

a 2 μm Si-doped n-type GaN, five periods of InGaN/GaN multiquantum well structures for emission maximum at 460 nm, and a Mg-doped p-type GaN layer were subsequently grown under normal conditions. Note that a highly Mg-doped p-type GaN (p^{++}-type GaN) layer was not adopted in our epitaxial structure. The samples were partially dry-etched to have a chip size of 500 × 700 μm^2. The SiO_2 was then removed by dipping the samples in a buffered oxide etching solution. Ni/Au (5 nm/5 nm) was deposited as a transparent conductive layer on the p-type GaN, and Cr/Au was applied for the metal contacts on the n- and p-type layers. A conventional LED without a GO stripe pattern was also fabricated under identical conditions for comparison, as shown in Figure 1a.

2.3. Characterization. The extent of GO reduction was studied by X-ray photoelectron spectroscopy (XPS) and Raman spectroscopy. The sheet resistance and resistivity were measured by using a four-point probe system and Hall effect measurement system at room temperature, respectively, and the surface morphology and thickness of the GO patterns were probed by atomic force microscopy (AFM). High-resolution transmission electron microscopy (HR-TEM) was used to verify the existence of reduced GO between GaN layers. Current−voltage (I−V) and light output−current (L−I) measurements were then carried out in a probe station system wired with a parameter analyzer.

3. RESULTS AND DISCUSSION

Figure 2 panels a and b show high-resolution C 1s spectra of the as-deposited and annealed GO sheet. The C 1s core level of the GO sheets is usually employed to confirm the extent of thermal reduction, that is, removal of the oxygen functional groups. As can be seen from Figure 2a, four peaks are clearly visible that can be assigned to carbon with different chemical valences, including nonoxygenated ring carbon (C−C, 284.6 eV), carbon in C−O bonds (286.6 eV), carbonyl bonds (C═O, 288.2 eV), and carboxylate bonds (O−C═O, 289.1 eV).[18] After thermal reduction, the intensity of the C−C peak clearly increased while the oxygen-related peaks decreased. The percentage of the C−C bond is estimated to be 83%, which is much higher than the value of 58% estimated for the as-deposited GO. This implies that most of the oxygen functional groups are removed during the high-temperature thermal annealing process. Furthermore, it is observed that the C−N bond (C−N, 285.7 eV) appears in the spectrum of reduced GO. The high-resolution N 1s spectrum (inset to Figure 2b) shows a single Gaussian-like peak centered at 398 eV, which corresponds to the C−N bonding state of carbon. This suggests that the ammonia gas likely acted as a dopant source during the thermal annealing process, as indicated in a previous study.[19] Raman spectra of the GO before and after thermal annealing are also compared in Figure 2c. Both spectra show two dominant bands at 1335 and 1586 cm^{-1}, which correspond to D and G bands of graphene oxide, respectively.[20] The D band arises from the structural imperfections of the edge planes and disordered structures in the A_{1g} mode. The G band corresponds to the first-order scattering of the E_{2g} mode and the ordered sp^2-bonded carbon. It should be noted that there is no frequency shift of the D and G bands after thermal annealing. From Figure 2c, the I_D/I_G intensity ratio before and after thermal annealing is estimated to be 1.06 and 1.14, respectively, which correspond to a mean sp^2 GO domain size (or interdefect distance, L_a) of ∼15.87 and 14.75 nm, estimated by using the empirical relation L_a (nanometers) = $(2.4 \times 10^{-10})\lambda_l^4(I_D/I_G)^{-1}$, where λ_l is the laser line wavelength used in the Raman experiment in nanometer units.[21] It indicates a slight decrease in the average size of the sp^2 GO domain upon thermal annealing, suggesting that the oxygen functional groups attached to the edge of the aromatic domain are eliminated from GO sheets through thermal annealing.[22]

The sheet resistance and electrical resistivity of the reduced GO measured for different GO thicknesses by four-point probe and Hall effect measurements are presented in Figure 2d. The as-deposited GO is known to be an insulator, but the reduced GO sheets have electrical conductivity because the oxygen functional groups were removed. The sheet resistance and resistivity of a 10 nm reduced GO are measured to be 3.4 kΩ/□ and 4.1 × 10^{-3} Ω·cm, respectively. Also, the sheet resistances of reduced GO films of thicknesses 15 and 20 nm are measured to be 2.9 and 2.65 kΩ/□, respectively. This result shows an exponential decrease of sheet resistance with the film thickness, suggesting that the oxygen functional groups are removed differently depending on the thickness during the annealing process, and the C/O ratio decreases for a thicker GO sample. Indeed, Zhang et al.[23] previously reported on a decrease in the sheet resistance as the C/O ratio increased for reduced GO. The electrical properties in Figure 2d can be attributed to the combined effect of two factors: namely, thickness-dependent and oxygen functional group-dependent behavior. In addition, the N atoms were incorporated into the reduced GO network, as confirmed by XPS measurements (Figure 2b), forming a C−N bond at the edge site of the reduced GO. In fact, doping with electron-rich N atoms led to a decrease in the sheet resistance.[16] Based on all these combined effects, the reduced GO sheet shows very low resistivity (∼4.1

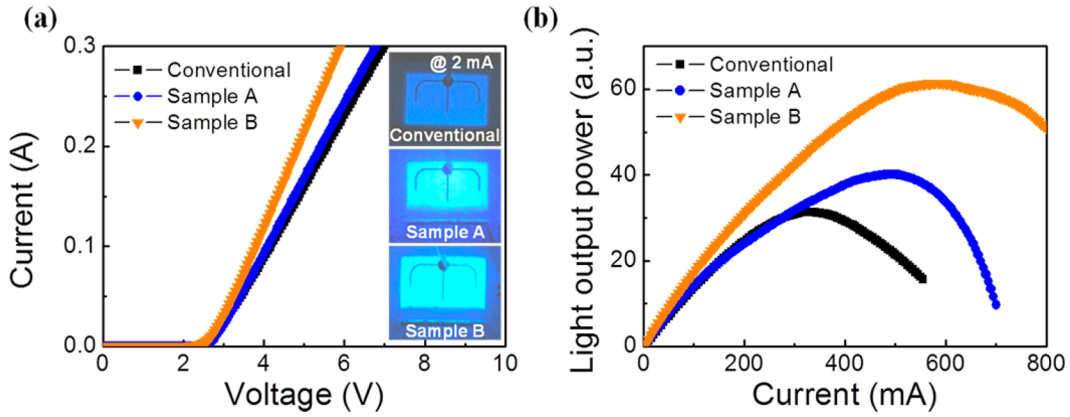

Figure 4. (a) $I-V$ and (b) light-output power versus current of the conventional LED, sample A, and sample B. (Inset) Optical microscopic images of the three respective devices during light emission at 2 mA.

$\times 10^{-3}$ Ω·cm), opening the potential application like the current-spreading layer for GaN-based LEDs.

The optical microscopic image of the patterned GO is shown in Figure 3a. The stripe and the electrode pattern are uniformly covered with GO sheets over a large area. AFM is used to characterize the reduced GO surface morphology, as shown in Figure S1 (Supporting Information). The surface is seen to have many wrinkles/folds formed during the spray-coating process. The as-deposited GO has a thickness of ∼13 nm, which after thermal reduction is reduced down to 10 nm, as shown in the inset to Figure S1. The decrease in the reduced GO film thickness (down by ∼3 nm) and surface roughness (from 3.4 to 1.2 nm) after thermal reduction implies that the oxygen functional groups are significantly removed. The HR-TEM image shows that the reduced GO is embedded between GaN layers, as shown in Figure 3b and Figure S2 (Supporting Information). From the average profile of intensity analysis, the thickness of the embedded reduced GO was estimated to be ∼10 nm, which is consistent with the AFM results.

Figure 4a shows the $I-V$ characteristics of the fabricated LEDs. The forward voltages (V_f) at 100 mA for the conventional device, sample A, and sample B are measured to be 4.15, 4.1, and 3.8 V, respectively. This result shows a significant improvement in the device V_f for sample B, while the conventional device and sample A have nearly similar V_f values. Furthermore, the slope of the $I-V$ curve of sample B is very steep as compared to other two samples, especially at high injection currents. To explain this observation, the series resistances (R_s) of the devices were calculated by using the equation $I(dV/dI) = (nkT/q) + R_sI$, where n is the ideality factor, k is the Boltzmann constant, T is the temperature, and q is the elementary charge.[24] The estimated R_s values (see Figure S3 in Supporting Information) are 15.9, 14.5, and 10.7 Ω for the conventional device, sample A, and sample B, respectively. Considering that the vertical resistance across the metal/p-type GaN interface in all our devices is expected to be similar, the low series resistance observed for sample B could be ascribed exclusively to introduction of the reduced GO layer and resistivity of the n-type GaN. To better understand this result, the specific contact resistance (ρ_c) of n-contact layer in each device is measured by using the transmission line model (see Figure S4 in Supporting Information). For Au/Cr and Au/Cr/rGO contacts on undoped GaN, ρ_c is estimated to be 7.89×10^{-4} and 1.4×10^{-4} Ω·cm^2, respectively. For the same contacts on n-type GaN, the values are 2.91×10^{-5} and 1.22×10^{-5} Ω·cm^2. It shows that the contact resistance between the metal and the GaN is slightly improved by insertion of reduced GO layer. Since the resistivity of the reduced GO (∼4.1×10^{-3} Ω·cm) is lower than that of the n-type GaN (∼0.01 Ω·cm), we surmise that the embedded reduced GO acts as a highly conducting layer even though it is relatively thin (∼10 nm). However, additional factors such as thermal annealing induced changes in the interfacial quality, and crystal quality improvement due to epitaxial lateral overgrowth on rGO cannot be ruled out when considering the low series resistance observed in sample B.

Optical light emission images of the respective devices are provided in the inset to Figure 4a. One can clearly notice brighter light emission from samples A and B compared to the conventional LED. Figure 4b shows the light output power as a function of injection current. Clearly, the light output power is enhanced when the current-spreading rGO layer is inserted. The light output power of samples A and B is enhanced in the upper direction by 1.07 and 1.45 times at 100 mA as compared to the conventional LED. This result once again proves that the reduced GO layer helps to spread out the injected current in the lateral direction and consequently reduces the current crowding effect. In other words, the LED with an embedded reduced GO layer effectively enhances the injection current with a rather uniform current density over the entire emission area.

In order to verify the current-spreading ability of reduced GO layer, the reduced GO is formed on undoped and n-type GaN, followed by the deposition of Cr/Au planar parallel electrodes separated by a distance of 700 μm. It should be noted that undoped and n-type GaN without a GO layer were also fabricated under the same conditions for comparison. As shown in Figure 5, the metal contacts with reduced GO on undoped and n-type GaN exhibit ohmic behavior that can be attributed to the high interfacial quality between reduced GO and the layer underneath. For the undoped and n-type GaN without reduced GO, the current values at 1 V are estimated to be 12 and 30 mA, respectively, which further increases to 36 and 72 mA when the reduced GO is introduced between the metal and epilayers. The $I-V$ characteristics of the sample with reduced GO on the undoped GaN are similar to those of the sample made on the n-type GaN without reduced GO. This result can be attributed to the fact that the resistivity of the reduced GO layer is much smaller than that of the n-type GaN layer and so the current flow in the sample with reduced GO is highly comparable to the sample of n-type GaN without

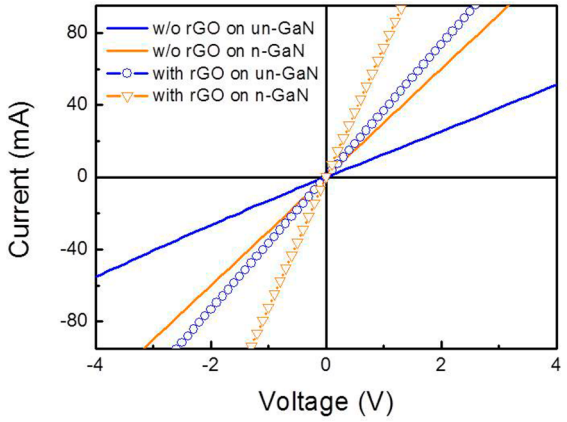

Figure 5. $I-V$ characteristics of Cr/Au contacts on undoped and n-type GaN with and without reduced GO sheet.

reduced GO.[10,25,26] In addition, the reduced GO on n-type GaN shows a further increase in current at any given voltage compared to the undoped GaN sample with reduced GO. This means that the enhanced $I-V$ characteristics of reduced GO on n-type GaN can be possible by the help of the low resistivity of n-type GaN, compared to undoped GaN.[27] Therefore, reduced GO, in spite of its thin nature, can be inferred to be suitable for use as a current-spreading layer in GaN-based LEDs.

It is well-known that current crowding at a high injection current accompanies a high series resistance, causing severe heating in the device with a high junction temperature (T_j). Figure 6 shows the estimated junction temperature (T_j) as a

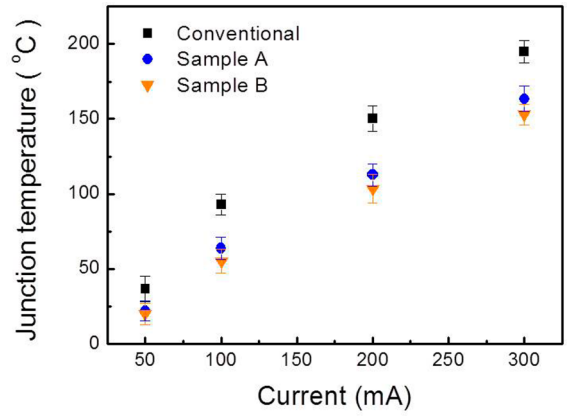

Figure 6. Junction temperature (T_j) as a function of injection current for the three different devices.

function of injection current at 300 K for the LEDs tested. The junction temperature of the LED devices was experimentally measured by using the forward voltage method, as described by Xi et al.[28] To investigate the thermal behavior of LEDs at high currents, the junction temperature is measured at different injection currents up to 300 mA. As expected, the junction temperature of the three samples linearly increases with the injection current. At an injection current of 300 mA, T_j is calculated to be 195 °C for the conventional LED, 163 °C for sample A, and 158 °C for sample B. It is apparent that there is a significant reduction in T_j for samples A and B compared to conventional LED. It is well documented that both the current crowding and self-heating effects could cause thermal rollover in LEDs at high injection currents. This can be understood by revisiting Figure 4b. The conventional LED having comparatively high series resistance and T_j undergoes thermal rollover at around 300 mA, whereas samples A and B having comparatively low series resistance and T_j appear to be able to give an uninterrupted emission increase up to 500 mA, above which the thermal rollover begins. It is therefore apparent that the reduced GO layer offers better current and heat spreading for the device by virtue of its high electrical and thermal conductivities.

4. CONCLUSIONS

The electrical and optical performance of GaN LEDs embedding a reduced GO sheet as a current spreader have been studied. The LED with reduced GO on the n-type GaN demonstrated significantly improved $L-I-V$ performance compared to an LED that had reduced GO on undoped GaN or a conventional device without reduced GO. Our results suggest that the reduced GO acts as a good current-spreading layer that circumvents the current crowding and thereby reduces the series resistance of the device. In addition, the junction temperature of the device with reduced GO was significantly reduced. The present study brings into the picture that embedded reduced graphene oxide can be used as a current- and heat-spreading layer in GaN LEDs for high-power and high-efficiency applications.

■ ASSOCIATED CONTENT

Supporting Information

Five figures showing surface morphology of reduced graphene oxide, TEM images of embedded reduced GO, series resistance and specific contact resistance of different devices, and schematic diagram of measuring structure. This material is available free of charge via the Internet at http://pubs.acs.org.

■ AUTHOR INFORMATION

Corresponding Author

*E-mail chhong@jbnu.ac.kr.

Author Contributions

The manuscript was written through contributions of all authors. All authors have given approval to the final version of the manuscript.

Notes

The authors declare no competing financial interest.

■ ACKNOWLEDGMENTS

This research was supported by Basic Science Research Program through the National Research Foundation of Korea (NRF) funded by the Ministry of Education (Grant 2013R1A1A2013044) and by Basic Science Research Program through the National Research Foundation of Korea (NRF) funded by the Ministry of Science, ICT & Future Planning (2010-0019694).

■ REFERENCES

(1) Nakamura, S.; Fasol, G. The Blue Laser Diode; Springer: New York, 1997.

(2) Schubert, E. F.; Kim, J. K. Solid-State Light Sources Getting Smart. *Science* **2005**, *308*, 1274−1278.

(3) Guo, X.; Schubert, E. F. Current Crowding and Optical Saturation Effects in GaInN/GaN Light-Emitting Diodes Grown on Insulating Substrates. *Appl. Phys. Lett.* **2001**, *78*, 3337−3339.

(4) Cho, J.; Schubert, E. F.; Kim, J. K. Efficiency Droop in Light-Emitting Diodes: Challenges and Countermeasures. *Laser Photonics Rev.* **2013**, *7*, 408−421.
(5) Kim, H.; Lee, S.-N. Theoretical Considerations on Current Spreading in GaN-based Light-Emitting Diodes Fabricated with Top-Emission Geometry. *J. Electrochem. Soc.* **2010**, *157*, H562−H564.
(6) Ryu, H.-Y.; Shim, J.-I. Effect of Current Spreading on the Efficiency Droop of InGaN Light-Emitting Diodes. *Opt. Express* **2011**, *19*, 2886−2894.
(7) Monemar, B.; Sernelius, B. E. Defect Related Issues in the "Current Roll-Off" in InGaN Based Light Emitting Diodes. *Appl. Phys. Lett.* **2007**, *91*, 181103.
(8) Geim, A. K.; Novoselov, K. S. The Rise of Graphene. *Nat. Mater.* **2007**, *6*, 183−191.
(9) Yan, Z.; Liu, G.; Khan, J. M.; Balandin, A. A. Graphene Quilts for Thermal Management of High-Power GaN Transistors. *Nat. Commun.* **2012**, *3*, 1−8.
(10) Chandramohan, S.; Kang, J. H.; Ryu, B. D.; Yang, J. H.; Kim, S.; Kim, H.; Park, J. B.; Kim, T. Y.; Cho, B. J.; Suh, E.-K.; Hong, C.-H. Impact of Interlayer Processing Conditions on the Performance of GaN Light-Emitting Diode with Specific NiO_x/Graphene Electrode. *ACS Appl. Mater. Interfaces* **2013**, *5*, 958−964.
(11) Pei, S.; Cheng, H.-M. The Reduction of Graphene Oxide. *Carbon* **2012**, *50*, 3210−3228.
(12) Han, N.; Cuong, T. V.; Han, M.; Ryu, B. D.; Chandramohan, S.; Park, J. B.; Kang, J. H.; Park, Y.-J.; Ko, K. B.; Kim, H. Y.; Kim, H. K.; Ryu, J. H.; Katharria, Y. S.; Choi, C.-J.; Hong, C.-H. Improved Heat Dissipation in Gallium Nitride Light-Emitting Diodes with Embedded Graphene Oxide Pattern. *Nat. Commun.* **2013**, *4*, 1452.
(13) Kumar, P. V.; Bernardi, M.; Grossman, J. C. The Impact of Functionalization on the Stability, Work Function, and Photoluminescence of Reduced Graphene Oxide. *ACS Nano* **2013**, *7*, 1638−1645.
(14) Ryu, B. D.; Han, N.; Han, M.; Chandramohan, S.; Park, Y. J.; Ko, K. B.; Park, J. B.; Cuong, T. V.; Hong, C.-H. Stimulated N-doping of Reduced Graphene Oxide on GaN under Excimer Laser Reduction Process. *Mater. Lett.* **2014**, *116*, 412−415.
(15) Compton, O. C.; Nguyen, S. T. Graphene Oxide, Highly Reduced Graphene Oxide, and Graphene: Versatile Building Blocks for Carbon-Based Materials. *Small* **2010**, *6*, 711−723.
(16) Chitara, B.; Krupanidhi, S. B.; Rao, C. N. R. Solution Processed Reduced Graphene Oxide Ultraviolet Detector. *Appl. Phys. Lett.* **2011**, *99*, No. 113114.
(17) Yang, D.; Zhou, L.; Chen, L.; Zhao, B.; Zhang, J.; Li, C. Chemically Modified Graphene Oxides as a Hole Transport Layer in Organic Solar Cells. *Chem. Commun.* **2012**, *48*, 8078−8080.
(18) Wei, D.; Liu, Y.; Wang, Y.; Zhang, H.; Huang, L.; Yu, G. Synthesis of N-Doped Graphene by Chemical Vapor Deposition and Its Electrical Properties. *Nano Lett.* **2009**, *9*, 1752−1758.
(19) Yan, Q.; Huang, B.; Yu, J.; Zheng, F.; Zang, J.; Wu, J.; Gu, B.-L.; Liu, F.; Duan, W. Intrinsic Current−Voltage Characteristics of Graphene Nanoribbon Transistors and Effect of Edge Doping. *Nano Lett.* **2007**, *7*, 1469−1473.
(20) Akhavan, O. The Effect of Heat Treatment on Formation of Graphene Thin Films from Graphene Oxide Nanosheets. *Carbon* **2010**, *48*, 509−519.
(21) Cançado, L. G.; Takai, K.; Enoki, T.; Endo, M.; Kim, Y. A.; Mizusaki, H.; Jorio, A.; Coelho, L. N.; Magalhães-Paniago, R.; Pimenta, M. A. General Equation for the Determination of the Crystallite Size La of Nanographite by Raman Spectroscopy. *Appl. Phys. Lett.* **2006**, *88*, No. 163106.
(22) Dong, X.; Su, C.-Y.; Zhang, W.; Zhao, J.; Ling, Q.; Chen, P.; Li, L.-J. Ultra-Large Single-Layer Graphene Obtained from Solution Chemical Reduction and Its Electrical Properties. *Phys. Chem. Chem. Phys.* **2010**, *12*, 2164−2169.
(23) Zhang, B.; Li, L.; Wang, Z.; Xie, S.; Zhnag, Y.; Shen, Y.; Yu, M.; Deng, B.; Huang, Q.; Fan, C.; Li, J. Radiation Induced Reduction: An Effective and Clean Route to Synthesize Functionalized Graphene. *J. Mater. Chem.* **2012**, *22*, 7775−7781.
(24) Shan, Q.; Meyaard, D. S.; Dai, Q.; Cho, J.; Schubert, E. F.; Son, J. K.; Sone, C. Transport-Mechanism Analysis of the Reverse Leakage Current in GaInN Light-Emitting Diodes. *Appl. Phys. Lett.* **2011**, *99*, No. 253506.
(25) Zhang, S. G.; Zhang, X. W.; Si, F. T.; Dong, J. J.; Wang, J. X.; Liu, X.; Yin, Z. G.; Gao, H. L. Ordered ZnO Nanorods-Based Heterojunction Light-Emitting Diodes with Graphene Current Spreading Layer. *Appl. Phys. Lett.* **2012**, *101*, No. 121104.
(26) Kim, B. J.; Lee, C.; Jung, Y.; Baik, K. H.; Mastro, M. A.; Hite, J. K.; Eddy, C. R., Jr.; Kim, J. Large-Area Transparent Conductive Few-Layer Graphene Electrode in GaN-Based Ultra-Violet Light-Emitting Diodes. *Appl. Phys. Lett.* **2011**, *99*, No. 143101.
(27) Su, Y. K.; Chang, S. J.; Wei, S. C.; Chuang, R. W.; Chen, S. M.; Li, W. L. Nitride-Based LEDs with n-GaN Current Spreading Layers. *IEEE Electron Device Lett.* **2005**, *26*, 891−893.
(28) Xi, Y.; Xi, J.-Q.; Gessmann, T.; Shah, J. M.; Kim, J. K.; Schubert, E. F.; Fischer, A. J.; Crawford, M. H.; Bogart, K. H. A.; Allerman, A. A. Junction Temperature Measurements in Deep-UV Light-Emitting Diodes using Three Different Methods. *Appl. Phys. Lett.* **2005**, *86*, No. 031907.